Estimation of Respiration Rate from Three-Dimensional Acceleration Data Based on Body Sensor Network

Guan-Zheng Liu, Ph.D.,[1–3] Yan-Wei Guo, Ph.D.,[1,3] Qing-Song Zhu, M.S.,[1,3] Bang-Yu Huang, M.S.,[1,3] and Lei Wang, Ph.D.[1,3]

[1]*Institute of Biomedical and Health Engineering, Shenzhen Institutes of Advanced Technology, Chinese Academy of Sciences, Shenzhen, China.*
[2]*Biomedical Engineering Program, Sun Yat-sen University, Guangzhou, China.*
[3]*Key Lab of Health Informatics, Chinese Academy of Sciences, Shenzhen, China.*

Abstract

Respiratory monitoring is widely used in clinical and healthcare practice to detect abnormal cardiopulmonary function during ordinary and routine activities. There are several approaches to estimate respiratory rate, including accelerometer(s) worn on the torso that are capable of sensing the inclination changes due to breathing. In this article, we present an adaptive band-pass filtering method combined with principal component analysis to derive the respiratory rate from three-dimensional acceleration data, using a body sensor network platform previously developed by us. In situ *experiments with 12 subjects indicated that our method was capable of offering dynamic respiration rate estimation during various body activities such as sitting, walking, running, and sleeping. The experimental studies also suggested that our frequency spectrum-based method was more robust, resilient to motion artifact, and therefore outperformed those algorithms primarily based on spatial acceleration information.*

Key words: *dynamic respiratory monitoring, body sensor network, acceleration-derived respiration rate, home health monitoring*

Introduction

The necessity for early diagnosis of potentially dangerous conditions, such as sleep apnea[1], sudden infant death syndrome[2], and chronic obstructive pulmonary disease[3] has fostered the development of several methods for measuring respiratory activity, especially in ambulatory settings. As the gold standard, the capnograph device was routinely used in hospital and critical care centers to monitor patients' respiratory status.[4] Other well-accepted respiratory monitoring techniques and devices are respiratory inductive plethysmograph (RIP)[5], electrical impedance tomography[6], thermistors for airflow measurements[7], piezoelectric transducers, and micro-electromechanical systems (MEMS) accelerometers. Empowered by body sensor network (BSN) technology these methods became more easily to deploy while being less obtrusive to patients.[8,9] More recently, Baltag and Popa[10] designed a microwave Doppler transducer and Li et al.[11] proposed a radar-based approach for noninvasive respiratory monitoring, but their attempts are still premature for clinical employments.

Accelerometers have been increasingly used in recently years to derive respiration rate. Accelerometers worn on the torso are capable of measuring inclination and angular changes during breathing, and then respiratory rate can be estimated using digital signal processing technology. Hung et al.[12] proposed a new approach based on a chest biaxial accelerometer to derive respiratory rate during static body conditions (e.g., sitting, standing and lying down).[13] Anmin et al.[14] suggested a hybrid principal component analysis (PCA) method (using full angles and the PCA) to derive respiratory rate with a three-dimensional (3D) accelerometer during static body conditions. Bates et al.[15] presented a wireless 3D accelerometer device to derive respiration rate, which tracked the axis of rotation and obtained regular rates of breathing motion. The aforementioned methods mainly used spatial acceleration information. Therefore, when the subject was changing position, the respiration rate estimation inevitably deteriorated because the magnitude of the movement-induced signal greatly exceeds that due to breathing, and the posture and orientation of the 3D accelerometer shifted during the disturbance. To cancel these problems, these authors simply removed the acceleration signal episodes that were contaminated by motion artifacts.[14,15]

On another side of the spectrum, different frequency spectrum analysis algorithms were developed to derive respiration rate from various physiological signals such as electrocardiograph (ECG), piezoelectric pulse signal, and photoplethymograph (PPG). Band-pass filter[16] and Wavelet transform[17–19] were applied to derive respiratory rates from single-a lead ECG signal. Dash et al.[20] used a time–frequency analysis method to estimate the respiration rate from ECG, PPG, and piezoelectric pulse transducer signals. Chon et al.[21] used a time–frequency spectral method to estimate respiratory rate from PPG data. It is logical to attempt the spectrum analysis approach for respiration rate estimation from wearable acceleration signals.

This article briefly described a wearable device to sense the 3D acceleration. The device was based on a BSN platform developed by us in previous studies.[9] A novel spectrum analysis method was presented to derive respiration rate from 3D acceleration signals. Consequently, experimental studies were carried out to verify our method and conclusion was given at the end.

System and Methods

The complete system was comprised of hardware modules for 3D acceleration signal acquisition, signal processing algorithms for

energy expenditure (EE) estimation, and respiration rate estimation, as detailed below.

HARDWARE MODULES

The BSN platform included the node boards that serve as the primary BSN components; the RIP sensor interface board that interfaces with an RIP belt sensor, the ECG interface board that was capable of detecting heart rate from non-contact electrodes, a PPG sensor interface board that interfaces with a generic PPG sensor, a base station board that connects with a personal computer or a personal digital device; a battery board with a wireless charger that provides power supply for the node and sensor boards; and several prototyping boards for debugging purpose. A low-power microprocessor, a radio transceiver, a memory integrated circuit (IC), a 3D accelerometer, a power regulator, a 20-pin expansion port, and affiliated discrete components were integrated on the BSN node. An improved media access control (MAC) protocol was presented to facilitate wireless data communications, which solved collision voidance, message recovery, and power consumption bottlenecks. All the boards, except the base station board, were designed in a uniform form factor that is 23 mm in diameter. There are well-defined expansion ports in all, but the base station board so the boards could be easily stacked. As shown later the BSN modules were assembled as a waistband device for 3D acceleration signal monitoring. *Figure 1* illustrated the node board, the resiration belt, the mask, and the experiment setup for 3D acceleration data acquisition.

ACCELEROMETER

The detection of body motions is important for behavior profiling and biofeedback training.[22] A digital built-in 3-axis accelerometer SCA3000

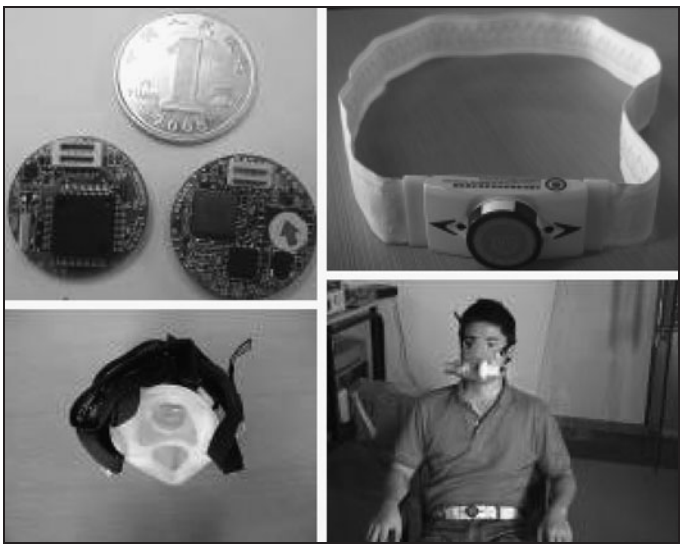

Fig. 1. The node boards for 3D acceleration detection (top, left); the abdomen belt for respration detection (top, right); a mask for BIOPAC CO_2 100C module (bottom, left), the experiment setup (bottom, right). 3D, three-dimensional.

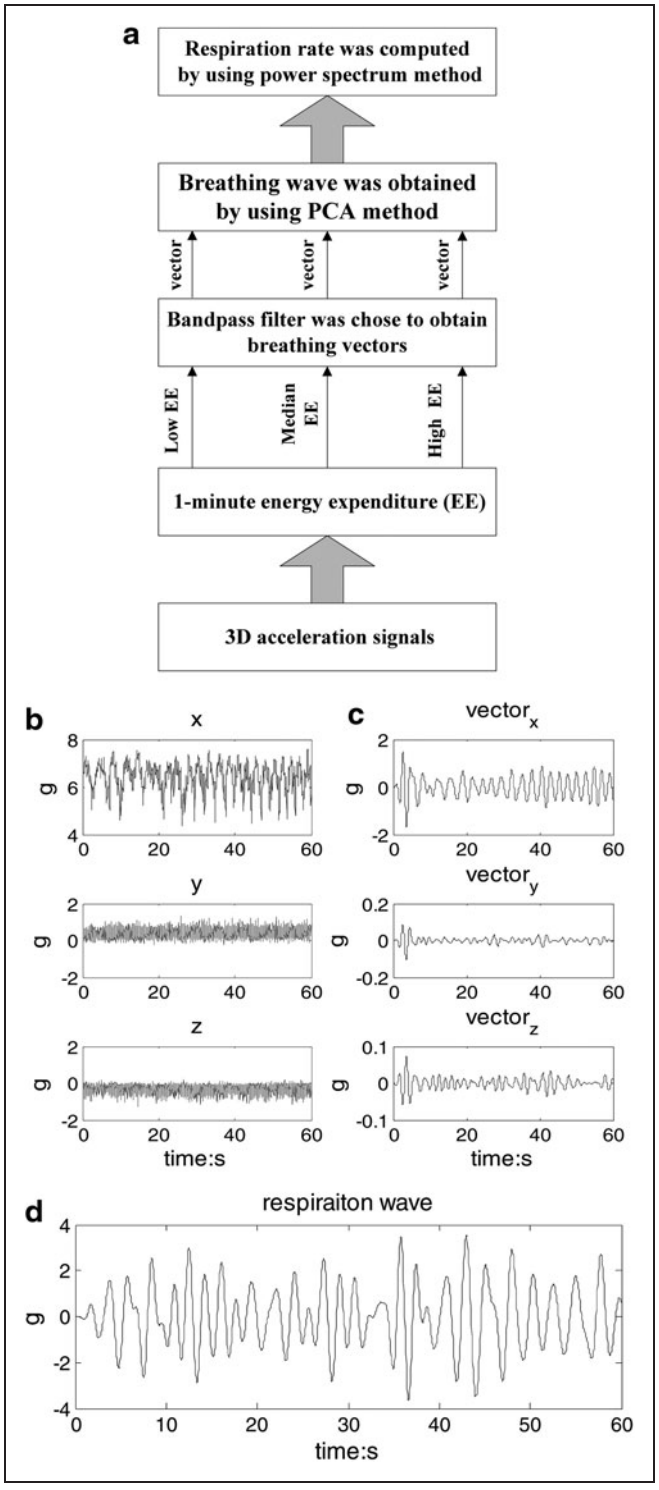

Fig. 2. (a) The step-by-step procedures for motion-derived respiratory rate estimation, **(b)** raw 3D acceleration signals for 1 min episode, **(c)** the three vectors derived from 3D acceleration signals by using the band-pass filter based on 1-minute EE, and **(d)** the respiration wave derived from three vectors by using the PCA method. EE, energy expenditure; PCA, principal component analysis.

was equipped in the node board. This device incorporates a 3D MEMS element and a signal conditioning application-specific integrated circuit (ASIC).[23] With its integrated design, the BSN node became more compact and immune to the noises induced by cables and connectors.

3D ACCELERATION-DERIVED RESPIRATION RATE

3D acceleration signals were monitored by the waist-worn device (*Fig. 1*) during various body activities. In general, abdomen motion includes body motion and respiration motion, and the frequency band for respiration ranged from 0.1 to 0.6 Hz during various body activities. The parameters of the band-pass filter were set, according to the EE for every minute. Consequently, the adaptive filter was used to obtain three respiration vectors from *x, y*, and *z* coordinates of the 3D acceleration signal, respectively. A PCA method was used to obtain the weight of each vector and to extract the respiration waveform. Finally, the respiration rate was estimated by power spectrum analysis. *Figure 2* demonstrated the procedures that respiration rate was derived from abdomen 3D acceleration signals during different body activities. The algorithm was detailed step by step, as below.

EE CALCULATION

Acceleration signals from the three axes were acquired at a sampling rate of 25 samples per second (Sps). Typically, the acceleration of a moving object consists of two parts: the gravity and acceleration caused by movements, which were called static accelerations and dynamic accelerations, respectively. It is the latter that was primarily concerned in our experiments. A high-pass filter (-3dB bandwidth was 1 Hz) was employed to eliminate the static portions. The acceleration signal Ai was defined as[24]:

$$\Delta A(i) = [(x(i+1) - x(i))^2 + (y(i+1) - y(i))^2 + (z(i+1) - z(i))^2]^{1/2} \quad (1)$$

The EE for the abdomenal part was calculated as:

$$EE = \sum \Delta A(i) \text{ over } 1 \text{ min} \quad (2)$$

The routine activities were classified based on EE as:
If $EE < 100$, the activity was considered to be with low EE;
If $100 \le EE < 400$, the activity was considered to be with median EE;
If $EE \ge 400$, the activity was considered to be with high EE;

Table 1. Bandpass Digital Filter Parameters

ABDOMEN MOTION EE	BODY ACTIVITIES	FREQUENCY BAND (HZ)	STOP BAND (HZ)	COEFFICIENT
Low EE	Sitting: 30 min sitting with minor movements Strict sitting: 5 min	0.2–0.4	0.15–0.45	Rp = 6 Rs = 15
	Sleeping: normal sleeping for a night	0.2–0.4	0.15–0.45	Rp = 6 Rs = 15
Median EE	Walking: 3 min slow walk with 2.5 km/h	0.2–0.6	0.15–0.65	Rp = 9 Rs = 15
High EE	Running: 5 min run with 6.0 km/h	0.3–0.7	0.2–0.8	Rp = 3 Rs = 15

EE, energy expenditure.

ADAPTIVE DIGITAL FILTER

The respiratory rate is approximately 0.1 to 0.6 Hz during different body activities. According to the different EE values conducted from abdomen motions, the parameters of Butterworth band-pass filter were adaptively selected to derive respiration vectors from *x, y*, and *z* co-ordinates of 3D acceleration signals, separately. The parameters of Butterworth digital filter are shown in *Table 1*; the pass-band ripple Rp denotes the maximum permissible pass-band loss in decibels, and the stop-band attenuation Rs denotes the number of decibels that the stop-band is down from the pass-band.

PRINCIPLE COMPONENT ANALYSIS

Because of the unpredicted posture changes during routine activities and the geometric deployment of the accelerometer, a PCA-based method was proposed to obtain the weight of the respiration vectors from the *x*-, *y*-, and *z*-axis accelerations.

Table 2. Motion-Derived Respiratory Rate Experiments with Abdomen Accelerometer

ACTIVITIES	PROTOCOL	GOLDEN STANDARD	MAINLY MOTION
Stationary activity	Strict sitting quietly for 5min	CO_2 analysis with Biopic $CO_2$100C module	abdomen motion
	Sitting with minor movements for 30 min		Body/abdomen
Dynamic activity	Walking for 3 min with 2 km/h		Body motion
	Running for 5 min with 6 km/h		Body motion
Sleeping	Sleeping for above 6 h		Body/Abdomen

PCA is generally used for dimension reduction of multivariate datasets.[25] In this article the implementation is as follows:

First, denoting the three co-ordinate acceleration vectors time series as matrix $\sum = \{\text{vector}_x(k); \text{vector}_y(k); \text{vector}_z(k)\}$.

Second, the eigenvectors and corresponding eigenvalues ($\lambda_1, \lambda_2, \lambda_3$) of $\sum$ was computed based on classic PCA method.

Third, the weights for three co-ordinate acceleration vectors were obtained as the following equations:

$$\eta_i = \frac{\lambda_i}{\lambda_1 + \lambda_2 + \lambda_3} \qquad (i = 1, 2, 3) \qquad (3)$$

At last, the x_0 represents the respiratory time sequence by

$$x_0 = \eta_1 vector_x + \eta_2 vector_y + \eta_3 vector_z \qquad (4)$$

Where the vector_x, vector_y, and vector_z denote the vectors from *x*, *y*, and *z* co-ordinates of 3D acceleration filtered using adaptive band-pass filter, respectively.

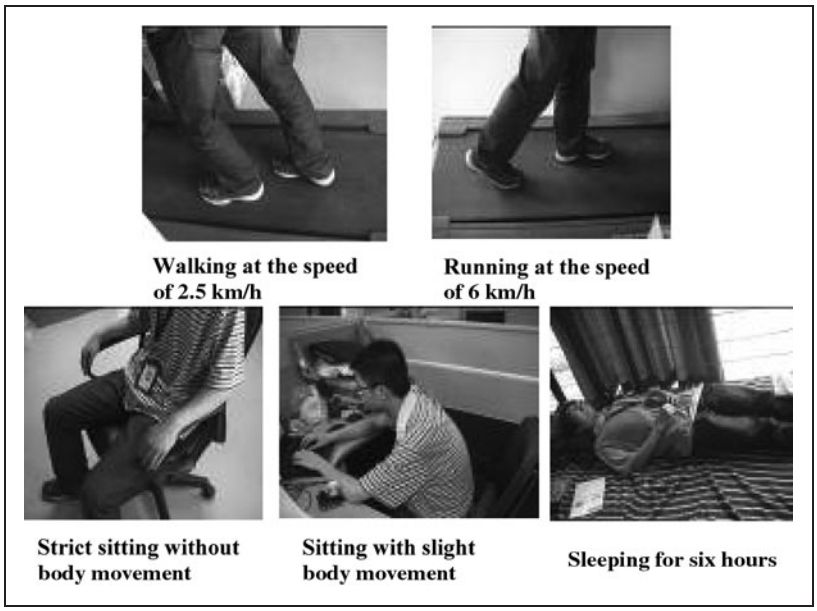

Fig. 3. The experiment circuit.

SPECTRUM ANALYSIS

Respiratory rate was estimated by using the power spectrum for every 1-min episode.

Experiment

PROTOCOL OF THE EXPERIMENT

Twelve healthy subjects with a mean age of 23.5 years (between 21 and 32) have participated in experiment 1 as shown in *Table 2*. All subjects were chosen randomly. The experiment protocol was illustrated in *Figure 3*:

The reference signal (being golden standard in our experiments) was obtained by the airflow CO_2 analysis with a BIOPAC CO_2 100C module (*Fig. 1*).

3D-ACCELERATION DERIVED RESPIRATION METHODS

To derive respiration rate from 3D acceleration signals, different methods based on wavelet decompositions acceleration-derived respiration (ADR)1–2 and nonadaptive band-pass filters (ADR3–4) were used, based on the indications in the literature of their potential merits and preliminary review of their implemented results.

(1) ADR1: respiration rate was derived by using wavelet decomposition, scale 6, and power spectrum from the 3D acceleration signals.
(2) ADR2: respiration rate was derived by wavelet decomposition, scale 5 plus scale 6, and power spectrum from the 3D acceleration signals.
(3) ADR3: respiration rate was derived with band-pass 0.2–0.8 Hz and power spectrum, from 3D acceleration signals.
(4) ADR4: respiration rate was derived with band-pass 0.2–0.6 Hz and power spectrum, from 3D acceleration signals.
(5) ADR5: our method, as detailed in the previous session.

STATISTICAL ANALYSIS

The accuracy of each method was estimated by the average percentage error of the measurements in comparison with the reference

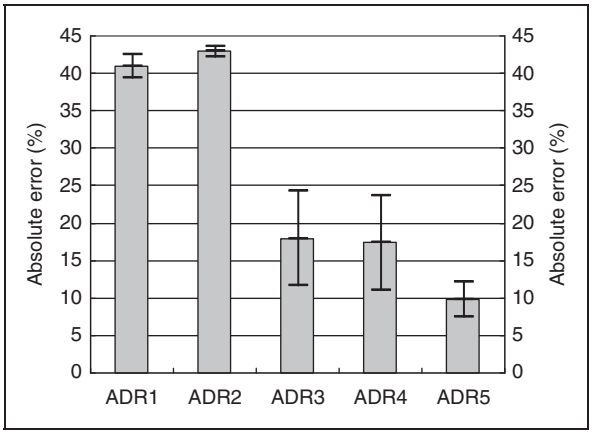

Fig. 4. The absolute error across all body activities (strict sitting, sitting with minor movement, walking, and running). Mean ± one standard deviation was plotted. ADR1–2 meant 3D-ADR rate based on wavelet; ADR3–4 meant 3D-ADR rate based on band-pass filter; ADR5 as detailed in the previous article. ADR, acceleration derived respiration.

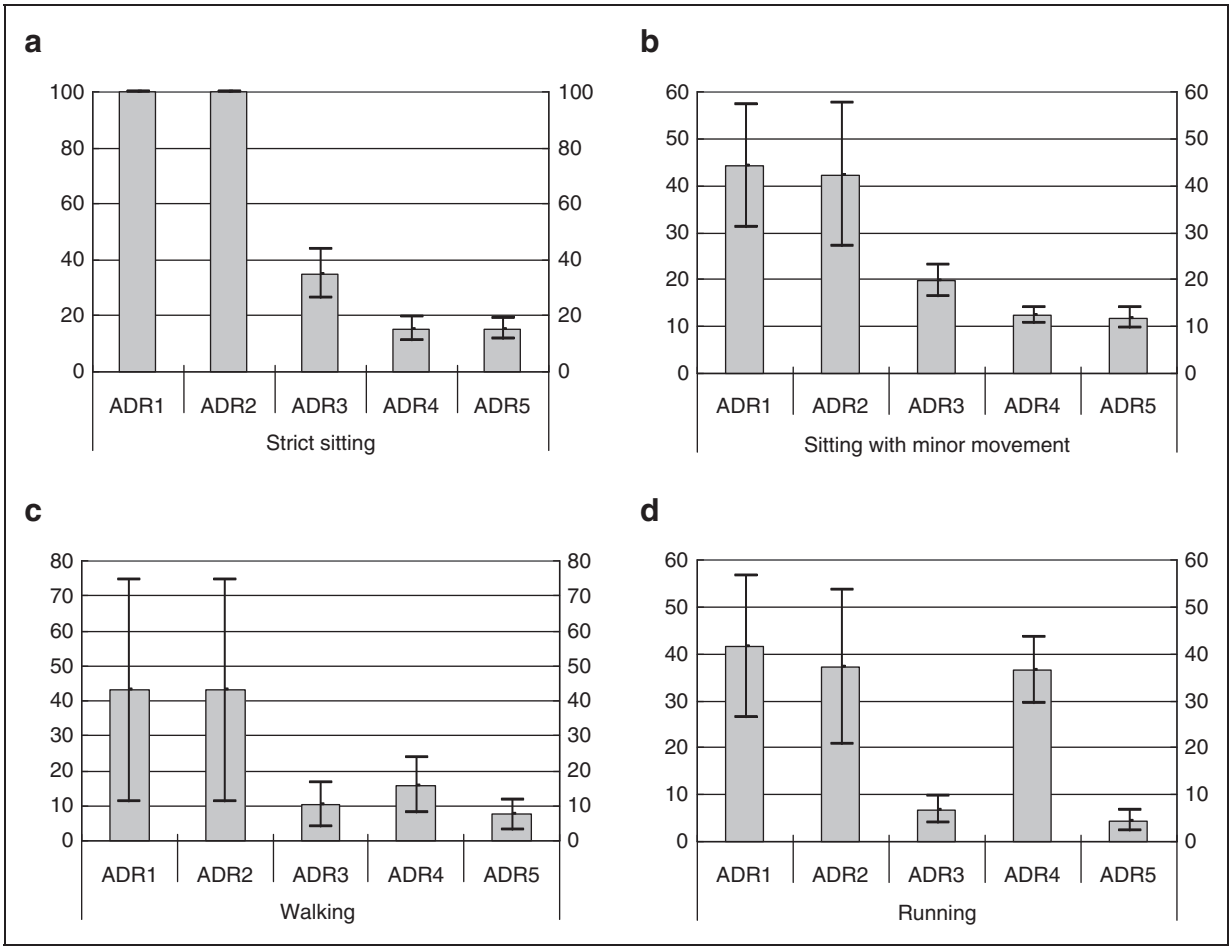

Fig. 5. The mean absolute errors of five methods during various body activates (e.g., strict sitting (**a**), sitting with minor movement (**b**), walking (**c**), and running (**d**)); Mean ± one standard deviation were plotted. ADR1–2 meant 3D-ADR rate based on wavelet; ADR3–4 meant 3D-ADR rate based on band-pass filter; ADR5 meant 3D-ADR rate based on PCA and band-pass filter that we designed in the article.

value, calculated by subtracting the test value from the reference value and dividing the results by the reference value of each measurement.[16] Absolute value was used in our study to minimize error offset between each experiment.

Table 3. Difference in Derived Respiratory Rate for Controlled 0.5-h Test

	DERIVED RESPIRATION METHODS: MEAN ± ONE STANDARD				
ACTIVITIES	ADR1	ADR2	AD3	ADR4	ADR5
Quiet	**100 ± 0**	**100 ± 0**	**34.86 ± 17.43**	15.36 ± 8.10	15.46 ± 7.67
Sitting	**44.26 ± 26.03**	**42.36 ± 30.67**	**19.85 ± 15.45**	12.39 ± 3.38	11.79 ± 4.35
Walking	**43.03 ± 63.22**	**42.83 ± 63.03**	10.35 ± 12.63	15.86 ± 15.59	7.45 ± 8.62
Running	**41.52 ± 30.29**	**37.32 ± 32.82**	6.79 ± 5.61	**36.62 ± 14.22**	4.52 ± 4.34

Mean absolute error difference with the reference value in breaths per minute (Bold values if significant difference with the reference value at $\alpha = 0.05$).

ADR, acceleration derived respiration.

$$Error = \frac{|(Derived - reference)|}{Observed} \times 100\ (\%) \quad (5)$$

$$\text{If } Error > 100, Error = 100 \quad (6)$$

We did the statistical tests (with SPSS v17.0) for all the experiments. Mean and standard deviations were used to evaluate the mean absolute error between the derived results and the reference values. Where two datasets were compared, we performed two sample *t*-tests for each individual method. The significance level was chosen as $\alpha = 0.05$.

Results

OVERALL PERFORMANCE OF ALL ACTIVITIES

Figure 4 depicts the mean absolute errors for the derived values and the

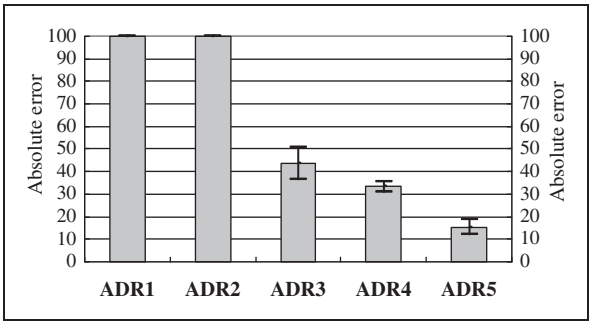

Fig. 6. The mean absolute error of ADR1–5 during sleeping. Mean ± one standard deviation were plotted. ADR1–2 meant 3D ADR rate based on wavelet; ADR3–4 meant 3D ADR rate based on band-pass filter; ADR5 meant 3D ADR rate based on PCA and band-pass filter in this article.

reference value during different body activities (strict sitting, sitting with minor movement, walking, and running). The result demonstrated that the ADR5 method achieved the least mean absolute error against the reference value at 10% approximately. The wavelet-based method (ADR1–2), which had the mean absolute error at 30%, had more significant difference with the reference value. The band-pass -based method (ADR3–4) had the mean absolute error at approximate 20%. This demonstrated that our method (ADR5) improved the measure accuracy, comparing with other methods.

PERFORMANCE FOR DIFFERENT ACTIVITIES

The dataset was partitioned into the following activity categories: strict sitting, sitting with minor movement, walking, and running. *Figure 5* indicates mean absolute differences for all methods. It is clear that the wavelet decomposition methods (ADR1 and ADR2) have the largest mean absolute error with the reference value during each body activity. However, The ADR5 method we have presented had the least mean absolute error with the reference value during each body activity. The band pass method (ADR3) had the similar performance to the ADR5 during walking and running, and the ADR4 had also the similar performance to the ADR5 during strict sitting and sitting with minor movement. The result demonstrated our algorithm improved the measure accuracy.

Table 3 demonstrates the difference in derived respiratory rate with reference value for all activities. Statistical testing shows that the wavelet methods (ADR1–2) had significant differences with the reference value at $\alpha = 0.05$ during each body activity. The ADR5 method did not have significant difference during each activity. The band-pass methods (ADR3–4) had significant differences with the reference value at $\alpha = 0.05$ during some activities, such as strict sitting (ADR3) and running (ADR4).

PERFORMANCE FOR OVERNIGHT MONITORING

Simultaneous respiratory and acceleration monitoring were performed for 10 subjects for overnight sleep monitoring. The result in *Figure 6* demonstrated that our algorithm outperformed the other data processing methods used in this article.

Discussion

An adaptive and frequency spectrum-based method was designed to estimate respiratory rate, because spatial acceleration information could be easily contaminated during various body activities. For example, Bates et al.[15] used a threshold method to remove contaminated acceleration signals and only 45% of the whole dataset was left for respiration rate estimation.[15] In contrast with Bates et al.[15] our algorithm was able to estimate respiration rate from the complete dataset without data tailoring. *Figure 7* summarized the magnitudes of the movement-induced signals during different body activities.

Denoting the respiration time series as x[k] and the reference signal as y[k], the correlation coefficient ρ_{xy} was calculated as

$$\rho_{xy} = \sum_{k=1}^{N-n} (x(k) - \overline{x(k)})(y(k+n) - \overline{y(k+n)}) \Big/ \sqrt{\sum_{k=1}^{N} (x(k) - \overline{x(k)})^2 \sum_{k=1}^{N} (y(k) - \overline{y(k)})^2} \quad (7)$$

Figure 8 indicates the variance of the correlation coefficient across all body activities, which suggested larger correlation coefficient during walking and running activities. This is because the frequency-domain expression (calculated with our ADR5 method) caused by respirations was enhanced due to physical exercise. This is clearly advantageous against those spatial acceleration-based methods, in which the correlation coefficient was reduced due to physical exercise.

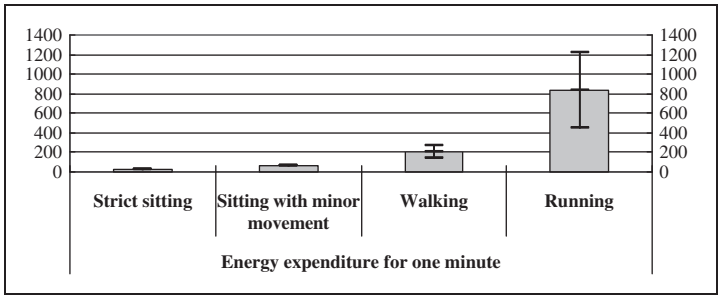

Fig. 7. EEs from abdomen motion during various body activities. Mean ± one standard deviation were plotted.

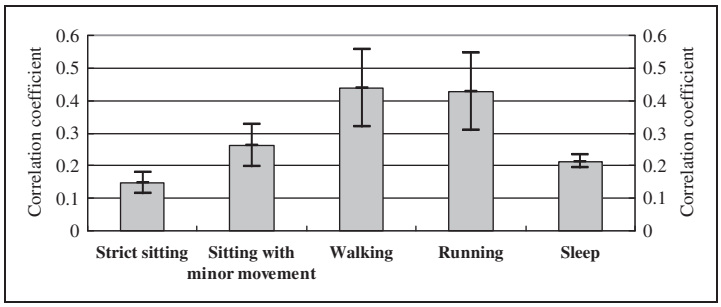

Fig. 8. Correlation coefficients between the outputs from the ADR5 method and the golden standard across all activities.

Conclusions

This article presents a respiration rate estimation method based on a generalized BSN development platform. The frequency spectrum-based algorithm, which combined PCA and adaptive band-pass filtering, was designed to derive respiration rate from 3D acceleration signal during various activities. *In situ* experiment results indicated our method was capable of offering pervasive respiration rate monitoring during various body activities. Furthermore, the result demonstrated that our method was more robust, resilient to motion artifact, and, therefore, outperformed those algorithms primarily based on spatial acceleration information. In the future we will investigate the long-term monitoring of the respiration rate using our method.

Disclosure Statement

No competing financial interests exist.

REFERENCES

1. Younes M. Role of respiratory control mechanisms in the pathogenesis of obstructive sleep disorders. *J Appl Physiol* **2008;**105:1389–1405.
2. Rantonen T, Jalonen J, Gronlund J, Antila K, Southall D, Valimaki I. Increased amplitude modulation of continuous respiration precedes sudden infant death syndrome-detection by spectral estimation of respirogram. *Early Hum Dev* **1998;**53:53–63.
3. Hasselgren M, Arne M, Lindahl A, Janson S, Lundback B. Estimated prevalence of respiratory syndromes, asthma and chromic obstructive pulmonary disease related to detection rate in primary health care. *Scand J Prim Heath Care* **2001;**9:54–57.
4. CO_2 module. Available at www.biopac.com (last accessed September 21, 2011).
5. Wu D, Wang L, Zhang YT. A wearable respiration monitoring system based on digital respiratory inductive plethysmography. In *Conf. 2009 IEEE Engineering in Medicine and Biology Society*. Minneapolis, MN: IEE, **2009;**4844–4847.
6. Woo EJ, Hua P, Webster JG, Tompkins WJ. Measuring lung receptivity using electrical impedance tomography. *IEEE Trans Biomed Eng* **1992;**39:756–760.
7. Nakajima K, Osa A, Miike H. A method for measuring respiration and physical activity in bed by optical flow analysis. *IEEE EMBC1997* **1997;**2054–2057.
8. Yang GZ. *Body sensor networks*. London: Springer-Verlag, **2006**.
9. Liu GZ, Huang BY, Wang L. A wearable respiratory biofeedback system based on generalized body sensor network. *Telemed J E Health* **2011;**17:348–357.
10. Baltag O, Popa GT. Microwaves doppler transducer for noninvasive monitoring of the cardiorespiratory activity. *IEEE Trans Magn* **2008;**44:4484–4487.
11. Li CZ, Cummings J, Lam J, Graves E, Wu WH. Radar remote monitoring of vital signs. *IEEE Microw Mag* **2009;**10:47–56.
12. Hung PD, Bonnet S, Gillemaud R, Castelli E, Yen PTN. Estimation of respiratory waveform using an accelerometer. *IEEE ISBI2008* **2008;**1493–1496.
13. Phan DH, Bonnet S, Guillemaud R, Castelli E, Pham NY. Estimation of respiratory waveform and heart rate using an accelerometer. In *Conference of 2008 IEEE Engineering in Medicine and Biology Society*. Vancouver, BC, Canada: IEE, **2008;**1–4.
14. Anmin J, Bin Y, Geert M, Haris D. Performance evaluation of a tri-axial accelerometry-based respiration monitoring for ambient assisted living. In *Conference of 2009 IEEE Engineering in Medicine Biology Society*. Minneapolis, MN: IEE, **2009;**1–4.
15. Bates A, Ling MJ, Mann J, Arvind DK. Respiratory rate and flow waveform estimation from tri-axial accelerometer data. In *Conference of 2010 IEEE Body Sensor Network*. Singapore: IEE, **2010;**1–7.
16. Boyle J, Bidargaddi N, Sarela A, Karunanithi M. Automatic detection of respiration rate from ambulatory single-lead ECG. *IEEE Trans Inf Technol Biomed* **2009;**13:890–896.
17. Roche F, Pichot V, Sforza E, Court-Fortune I, Duverney D, Costes F, Garet M, and Barthelemy JC. Predicting sleep apnoea syndrome from heart period: A time-frequency wavelet analysis, *Eur Respir J* **2003;**22:937–942.
18. Raymond B, Caytom R, Bates R, Chapell M. Screening for obstructive sleep apnoea based on the electrocardiogram-the computers in cardiology challenge. *Proc Comput Cardiol* **2000;**267–270.
19. Schrader M, Zywietz C, Von Einem V, Widiger B, Joseph G. Detection of sleep apnea in single channel ECGs from the PhysioNet data base. *Proc Comput Cardiol* **2000;**263–266.
20. Dash S, Shelley KH, Siverman DG, Chon KH. Estimation of respiratory rate from ECG, photoplethysmogram, and piezoelectric pulse transducer signals: A comparative study of time-frequency methods. *IEEE Trans Biomed Eng* **2010;**57:1099–1107.
21. Chon KH, Dash S, Ju KH. Estimation of respiratory rate from photoplethysmogram data using time-frequency spectral estimation. *IEEE Trans Biomed Eng* **2009;**56:2054–2063.
22. Aziz O, Wang L, Yang GZ, Darzi A. A pervasive body sensor network for measuring postoperative recovery at home. *Surg Innov* **2007;**14:83–90.
23. SCA3000-D01 3-AXIS LOW POWER ACCELEROMETER WITH DIGITAL SPI INTERFACE. VTI Technology. Available at www.vti.fi/en/ (ast accessed September 21, 2011).
24. Lin SJ, Wang L, Huang BY, Zhang YT, X. Wu M, Zhao JP. A pilot study on BSN-based ubiquitous energy expenditure monitoring. In *Conference of 2009 IEEE Body Sensor Networks*. Berkeley, CA: IEE, **2009;**1–4.
25. Duda RO, Hart PE, Stork DG. *Pattern classification*, 2nd ed. Beijing, China: China Machine Press and Citic Publishing House, **2003**.

Address correspondence to:
Lei Wang, Ph.D.
Institute of Biomedical and Health Engineering
Shenzhen Institutes of Advanced Technology
Key Lab of Health Informatics
Chinese Academy of Sciences
Shenzhen 518055
China

E-mail: wang.lei@siat.ac.cn

Received: January 29, 2011
Revised: April 17, 2011
Accepted: April 22, 2011